ORIGINAL RESEARCH

Rapeseed protein-derived antioxidant peptide RAP alleviates renal fibrosis through MAPK/NF-κB signaling pathways in diabetic nephropathy

Mingyan Zhang[1,*]
Zhibin Yan[1,*]
Lili Bu[1]
Chunmei An[2]
Dan Wang[1]
Xin Liu[1]
Jianfeng Zhang[1]
Wenle Yang[2]
Bochuan Deng[1]
Junqiu Xie[2]
Bangzhi Zhang[1,2]

[1]Institute of Biochemistry and Molecular Biology, School of Life Sciences, Lanzhou University, Lanzhou, China; [2]Key Laboratory of Preclinical Study for New Drugs of Gansu Province, School of Basic Medical Sciences, Lanzhou University, Lanzhou, China

*These authors contributed equally to this work

Correspondence: Junqiu Xie
School of Basic Medical Sciences, Lanzhou University, 199 Dong Gang West Road, Lanzhou 730000, China
Tel +86 931 891 5522
Fax +86 931 891 1255
Email xiejq@lzu.edu.cn

Bangzhi Zhang
School of Life Sciences, Lanzhou University, 222 Tian Shui South Road, Lanzhou 730000, China
Email zhangbz@lzu.edu.cn

Introduction: Kidney fibrosis is the main pathologic change in diabetic nephropathy (DN), which is the major cause of end-stage renal disease. Current therapeutic strategies slow down but cannot reverse the progression of renal dysfunction in DN. Plant-derived bioactive peptides in foodstuffs are widely used in many fields because of their potential pharmaceutical and nutraceutical benefits. However, this type of peptide has not yet been studied in renal fibrosis of DN. Previous studies have indicated that the peptide YWDHNNPQIR (named RAP), a natural peptide derived from rapeseed protein, has an antioxidative stress effect. The oxidative stress is believed to be associated with DN. The aim of this study was to evaluate the pharmacologic effects of RAP against renal fibrosis of DN and high glucose (HG)-induced mesangial dysfunction.

Materials and methods: Diabetes was induced by streptozotocin and high-fat diet in C57BL/6 mice and these mice were treated by subcutaneous injection of different doses of RAP (0.1 mg/kg and 0.5 mg/kg, every other day) or PBS for 12 weeks. Later, functional and histopathologic analyses were performed. Parallel experiments verifying the molecular mechanism by which RAP alleviates DN were carried out in HG-induced mesangial cells (MCs).

Results: RAP improved the renal function indices, including 24-h albuminuria, triglyceride, serum creatinine, and blood urea nitrogen levels, but did not lower blood glucose levels in DN mice. RAP also simultaneously attenuated extracellular matrix accumulation in DN mice and HG-induced MCs. Furthermore, RAP reduced HG-induced cell proliferation, but it showed no toxicity in MCs. Additionally, RAP inhibited the mitogen-activated protein kinase (MAPK) and nuclear factor κB (NF-κB) signaling pathways.

Conclusion: RAP can attenuate fibrosis in vivo and in vitro by antagonizing the MAPK and NF-κB pathways.

Keywords: antioxidant peptide, RAP, diabetic nephropathy, extracellular matrix, kidney fibrosis, MAPK, NF-κB

Introduction

Recent changes in lifestyle and eating habits have correlated with increased morbidity of diabetes year by year. Although drugs for treating blood glucose and blood pressure control have been developed,[1] the incidence of various chronic complications of diabetes has significantly increased. Diabetic nephropathy (DN) is a critical diabetic complication. It is the major cause of end-stage renal disease (ESRD), and it cannot be easily relieved by strict glycemic control alone.[2,3] Kidney fibrosis is the main pathologic change in DN, which eventually leads to ESRD.[4]

DN is a complex syndrome, and its pathogenesis includes loss of podocytes, mesangial cell (MC) hypertrophy, and thickening of the glomerular basement membrane

(GBM), which eventually leads to renal fibrosis.[5,6] Renal fibrosis is a consequence of the chronic inflammatory response caused by the release of several molecules, including growth factors, fibrogenic cytokines, and angiogenic factors. These molecules activate the excessive accumulation of extracellular matrix (ECM) in tissue, including collagens, α-smooth muscle actin (α-SMA), and fibronectin (FN), through epithelial-to-mesenchymal transition (EMT), which results in progressive renal dysfunction and organ failure.[7] High glucose (HG), oxidative stress, and transforming growth factor-β1 (TGF-β1) are mediators of renal injury and fibrosis in diabetes,[8] and connective tissue growth factor (CTGF), a prosclerotic cytokine acting downstream of TGF-β1, also plays a major role in the development of glomerulosclerosis and tubulointerstitial injury in DN.[9–11] Mitogen-activated protein kinases (MAPKs; mainly include ERK1/2 and p38) are involved in both normal renal physiology and in the pathology of various forms of kidney injury, including renal fibrosis.[12] It has also been demonstrated that MAPK plays an important role in the upregulation of TGF-β1 production in renal cell types[13] and contributes to the TGF-β1-induced transition of epithelial cells into myofibroblasts.[14–17] Activated MAPK is thought to be the physiologic activator of the nuclear transcription factor nuclear factor κB (NF-κB). NF-κB participates in processes that lead to kidney damage and renal interstitial fibrosis.[18] In diabetes, activated NF-κB translocates into the nucleus and triggers the excessive expression of its downstream target gene TGF-β1, causing ECM accumulation and renal fibrosis.[19,20] Consequently, it is possible to improve renal fibrosis caused by DN by reducing MAPK and NF-κB signaling in the kidney.

Currently, the strategy of DN treatment is to control blood sugar, reduce urinary protein, lower blood pressure, and control hyperlipidemia.[21] Existing treatments may slow down the progression of DN, but they cannot stop ESRD from occurring and causing side effects. Naturally extracted and sublimated bioactive peptides are a particularly significant component of functional foods. Inspection of crop proteomic data revealed that at least 6,000 proteins may have bioactive peptides. Much of the interest in these peptides is due to their potential pharmaceutical and nutraceutical benefits.[22,23] Some of the benefits to human health attributed to plant peptides are antibiosis, a reduction in blood cholesterol level, a reduction in blood pressure, antithrombosis, antioxidation, and opioid activity.[24–27] However, the effects of this type of peptides on DN and renal fibrosis have not been reported. Peptide YWDHNNPQIR (named RAP) is a natural peptide derived from rapeseed protein, and it confers resistance to oxidative stress.[28] The significance of oxidative stress in DN

is underscored by the finding that suppressing oxidative stress alleviates the manifestations associated with streptozotocin (STZ)-induced DN.[29] In this study, we tested the therapeutic effects of RAP on STZ-induced diabetic mice fed with a high-fat diet (HFD) and on HG-induced glomerular MC lines. Moreover, we investigated the molecular mechanism by which RAP protects against renal fibrosis in DN.

Materials and methods
Materials and reagents
DMEM was purchased from Gibco Invitrogen Corporation (Carlsbad, CA, USA). STZ was obtained from Sigma (Saint Louis, MO, USA). Fetal bovine serum (FBS) was purchased from Biological Industries (BI, Beit HaEmek, Israel). Mouse and rat enzyme-linked immunosorbent assay (ELISA) kits were obtained from Elabscience Biotechnology (Wuhan, China). Antibodies were purchased from the following sources: anti-FN antibody, anti-TGF-β1 antibody, and anti-CTGF antibody were from Abcam (Cambridge, UK); anti-p-Akt1/2, anti-Akt1/2, anti-NF-κB p-p65, anti-p38, and anti p-p38 antibody were from Cell Signaling Technology, Inc. (Beverly, MA, USA); anti-α-SMA antibody was purchased from Gene Tex Inc. (Alton Parkway Irvine, CA, USA); and anti-α-tubulin monoclonal antibody was from Proteintech Group, Inc. (Chicago, USA). IRDye 680LT goat anti-mouse immunoglobulin G (IgG) and anti-rabbit IgG were obtained from LI-COR Biosciences (Lincoln, NE, USA).

Synthesis of peptide RAP
The peptide RAP was synthesized on a p-methylbenzhydrylamine resin using the standard Fmoc-chemistry-based strategy. The final cleavage was performed using the standard protocol (95% trifluoroacetic acid/2.5% water/2.5% triisopropylsilane) for 3 h at room temperature. The peptide was purified and analyzed by reversed-phase high-performance liquid chromatography on a C18 column and characterized by electrospray ionization mass spectrometry. The RAP sequence is YWDHNNPQIR.

Animals
All animal experiments were performed in strict accordance with the Guide for the Care and Use of Laboratory Animals of the National Institutes of Health. The official procedure was approved by the Ethics Committee of Lanzhou University (Permit Number: SYXK Gan 2013-0003), China. Eight-week-old male C57BL/6 mice (20–25 g) were supplied by the Beijing Vital River Laboratory Animal Technology Co., Ltd. (Beijing, China). All mice were housed in a specific

pathogen-free laboratory under standard conditions in an air-conditioned room at 22°C±2°C under a 12-h light/12-h dark photoperiod with a relative humidity of 58%±10%. Mice were allowed access to a standard pelleted diet and water ad libitum. All mice were acclimatized for 1 week before inducing the diabetic animal model.

Induction of diabetes nephropathy and treatment

Diabetes was induced by injecting STZ at a dosage of 45 mg/kg dissolved in freshly prepared ice-cold 0.1 M citrate buffer (pH 4.5) for 5 consecutive days. The blood glucose level was detected from the tail using the ACCU-CHEK Performa blood glucose monitoring system (Roche Diagnostics GmbH. Germany) 72 hours after STZ injection. Mice with fasting blood glucose (FBG) levels above 11.1 mM were considered to be diabetic. Next, mice were randomly assigned to four experimental groups: the normal control, diabetic control, diabetic + low-dose RAP (0.1 mg/kg/day), and diabetic + high-dose RAP (0.5 mg/kg/day) groups. Treatment was continued until the 12th week with free access to a HFD. In the RAP treatment group (n=8), mice were injected with RAP every 2 days. The same dose of PBS was injected in both the normal group (n=6) and diabetic group (n=8).

Tissue collection and sample preparation

After 12 weeks of treatment, all animals were housed in metabolic cages to allow 24-hour urine collection and measurement of 24-hour urine volume and albumin level. Before being weighed and killed, the mice were fasted overnight with access to only water. Blood was drawn from the retroorbital plexus, the serum was separated, and all kidneys were preserved. All samples were stored at −80°C before testing.

Serum biochemical assays

Blood serum levels of malondialdehyde (MDA), superoxide dismutase (SOD) activity, catalase (CAT) activity, triglyceride, serum creatinine (Cr), blood urea nitrogen (BUN), and 24-h albuminuria were measured using standard enzymatic procedures (Nanjing Jiancheng Bioengineering Institute, Nanjing, China) according to the manufacturer's protocol.

Histopathologic and immunohistochemical analysis of mouse kidney tissues

Kidney tissues were fixed in 10% phosphate-buffered formalin solution and embedded in paraffin. Paraffin sections (3–4 μm) were stained with H&E, periodic acid-silver methenamine (PASM), Masson's trichrome, and Sirius red. For immunohistochemical analysis, mouse kidney sections were separated, rehydrated, and incubated with anti-FN (1:200; Abcam, Cambridge, MA, USA), anti-α-SMA (1:500; GeneTex, Irvine, CA, USA), anti-TGF-β1, anti-CTGF (1:400; Abcam, Cambridge, MA, USA), anti-p-p65 (1:400; Cell Signaling Technology, MA, USA), anti-p-p38, and anti-p-ERK1/2 antibodies (1:400; Cell Signaling Technology, MA, USA). Then, the percentage of positively stained area was measured in high-power (×400) fields on each slide and quantified using Image-Pro Plus software.

Cell culture and stimulation

Rat glomerular MCs were purchased from Beijing North Carolina Souren Biotechnology Research Institute (Beijing, China) and cultured in low-glucose DMEM containing 10% FBS at 37°C and 5% CO_2. MCs between the fifth and eighth passages were used for all experiments. Cells were grown to confluence and synchronized in serum-free DMEM for 24 h. The medium was then changed to 1) DMEM containing 5.5 mM glucose (normal glucose, NG); 2) DMEM containing 22 mM glucose (HG); and 3–4) HG medium with different concentrations of RAP for 48 h.

Cell proliferation and cytotoxicity assay (MTT test)

The MTT assay was applied to detect cell proliferation and cytotoxicity. Briefly, cells were seeded at 10^4 cells/well in 96-well plates. Before experiments, cells were serum starved for 24 h. Next, cells were incubated with NG or NG with 50, 100, 150, 200, and 250 μM RAP, or cells were treated with NG, HG, or HG with or without 50 and 100 μM RAP for 48 h. Then, 20 μL of MTT (5 mg/mL) was added to each well and incubated at 37°C for an additional 4 h. The medium was carefully removed, dimethyl sulfoxide (150 μL) was added into each well, and the absorbance of solubilized blue formazan was read at a wavelength of 570 nm using a microplate reader.

Western blot analysis

Total protein was extracted from MCs or mouse kidney tissues, and protein concentrations were assessed using the BCA Protein Assay Kit (Applygen Technologies Inc., Beijing, China). Equal amounts of protein extracts were subjected to 10% sodium dodecyl sulfate-polyacrylamide gel electrophoresis and transferred onto polyvinylidene difluoride membranes (Millipore Corp., Bedford, MA, USA). Sliders were blocked with 5% bovine serum albumin in Tris-buffered saline containing Tween-20 (TBST, pH 7.6) for 2 h at room temperature,

and incubated with specific primary antibodies (FN, 1:500; TGF-β1, p-ERK1/2, ERK1/2, p-p65, p-p38, p-38 1:1,000; anti-a-Tubulin, 1:2,000) overnight at 4°C. The membranes were rinsed with TBST and then incubated with the appropriate fluorescent secondary antibodies (1:10,000; LI-COR Biosciences) for 1 h at room temperature with protection from light. The protein bands were captured and quantified using the Odyssey infrared imaging system (LI-COR Biosciences).

Quantitative real-time reverse transcriptase polymerase chain reaction (RT-PCR)

Total RNA was extracted from mouse kidney tissues or MCs with TRIzol reagent, and reverse transcribed with the reverse transcriptase kit. All kits were used according to the manufacturer's instructions (Takara Bio Inc., Kyoto, Japan). The resulting cDNAs were used for quantitative PCR using the Power SYBR® Green PCR Master Mix (Takara Bio Inc). Real-time quantitative PCR was carried out using the Roter Gene 3000 real time RT-PCR system (Corbett Bio Inc., Sydney, Australia), SYBR green master mix, and primers. Quantitation of the mRNA levels was performed using the $2^{-\Delta\Delta Ct}$ method and using glyceraldehyde-3-phosphate dehydrogenase as a housekeeping gene. The primer sequences used are provided in Table 1.

ELISA

MCs were grown in 24-well plates and cultured with different media at 37°C and 5% CO_2. After 48 h, the levels of FN and COL4 in the supernatant of MCs for each group were determined by using rat FN and COL4 ELISA kits (Wuhan Elabscience Biotechnology, Wuhan, China). In addition, the levels of TGF-β1 in the mouse blood serum were tested by using mouse TGF-β1 ELISA kits according to the manufacturer's instructions.

Statistical analysis

All the experiments were repeated at least in triplicate with similar results, and the results are presented as the mean ± SD. The means of every two groups were detected with unpaired Student's t-test. One-way analysis of variance was used for multiple-group comparison (GraphPad Prism 5.0, USA). $P<0.05$ was considered to be statistically significant.

Results

In vivo experiments

Effects of RAP on blood glucose levels and body weights (BWs) of diabetic mice

The blood glucose levels and BWs of experimental mice were measured before and after treatment with RAP. Compared to those of the normal control mice, the blood glucose levels of the diabetic mice were notably increased, and treatment with RAP for 12 weeks had no effect on the blood glucose levels of diabetic mice. Additionally, the BWs of diabetic mice decreased after STZ plus HFD treatment. However, RAP markedly ameliorated the loss of BW (Table 2).

RAP ameliorates biochemical indices, oxidative stress parameters, and serum TGF-β1 expression levels in diabetic mice

To evaluate renal dysfunction, we evaluated the renal functional parameters (serum Cr, BUN, and 24-h albuminuria) in experimental mice after treatment with RAP for 12 weeks. As shown in Figure 1, all parameters were significantly higher

Table 1 Primer sequences for real-time polymerase chain reaction

Genes	Forward primer (5′–3′)	Reverse primer (5′–3′)
Mouse		
FN	GATTGGCGACAAGTGGAG	TAGGTGAACGGGAGGACA
TGF-β1	ATGGTGGACCGCAACAAC	CCAAGGTAACGCCAGGAA
CTGF	GGGCCTCTTCTGCGATTTC	ATCCAGGCAAGTGCATTGGTA
α-SMA	ACTGGGACGACATGGAAAAG	CATCTCCAGAGTCCAGCACA
GAPDH	AGGAGTAAGAAACCCTGGAC	CTGGGATGGAATTGTGAG
Rat		
FN	CAGGGGAAGAAAAGGAGCCC	CACGAAGTGTGGTTCCCCTC
TGF-β1	TGACATGAACCGACCCTTCC	CCAGGCTCCAAATGTAGGGG
CTGF	TAGCAAGAGCTGGGTGTGTG	TTCACTTGCCACAAGCTGTC
α-SMA	ACTGGGACGACATGGAAAAG	CATCTCCAGAGTCCAGCACA
GAPDH	GTTACCAGGGCTGCCTTCTC	ACCAGCTTCCCATTCTCAGC

Abbreviations: CTGF, connective tissue growth factor; FN, fibronectin; IHC, immunohistochemistry; GAPDH, glyceraldehyde-3-phosphate dehydrogenase; α-SMA, α-smooth muscle actin; TGF-β1, transforming growth factor-β1.

Table 2 Effects of RAP on the fasting blood glucose levels and body weights of diabetic mice

Groups	Fasting blood glucose (mmol/L)		Body weights (g)	
	Before treatment	After treatment	Before treatment	After treatment
Control	7.93±0.62	7.45±0.76	22.91±2.19	28.473±1.27
DM	21.25±3.18###	19.68±2.97###	22.07±1.81	24.844±1.98#
DM+RAP-L	20.21±4.18	20.11±2.15	23.02±2.12	27.39±1.95*
DM+RAP-H	22.51±5.12	18.71±2.49	21.78±1.29	26.24±1.61*

Notes: Data are expressed as the mean ± SD; n=8. #$p<0.05$ and ###$p<0.001$, diabetic control versus normal control. *$p<0.05$, diabetic + RAP versus DM.
Abbreviations: DM, diabetic model; RAP-H, high-dose RAP; RAP-L, low-dose RAP.

in diabetic mice than in normal control mice. However, low-dose RAP treatment markedly reduced the 24-h albuminuria and BUN levels in diabetic mice but not the levels of serum Cr. High-dose RAP treatment dramatically reduced the serum Cr, BUN, and 24-h albuminuria levels in diabetic mice (Figure 1A–C). Furthermore, STZ-induced mice fed with HFD showed a sharp elevation in serum triglyceride. However, RAP-treated mice revealed a significant decline in serum triglyceride (Figure 1D). As a key mediator in renal fibrosis, the level of TGF-β1 in serum was measured using ELISA kits. The results showed that TGF-β1 was prominently upregulated in STZ-induced diabetic mice compared to normal mice. It was markedly decreased by RAP treatment in high doses (Figure 1E).

To determine the influence of RAP on oxidative stress factors, we measured the concentrations of MDA, SOD, and CAT in serum after treatment with RAP. The results showed that there was no statistically significant difference in CAT levels among the 4 treatment groups (Figure 1F). The concentration of MDA was higher and that of SOD was lower in DN mice than in normal mice. However, RAP treatment significantly downregulated the concentration of MDA and upregulated the concentration of SOD (Figure 1G and H), indicating efficient antioxidation in DN mice.

RAP inhibits the glomerular hypertrophy and GBM thickening in diabetic mice

To determine renal histopathologic changes, H&E and PASM staining were used to observe glomerular hypertrophy and GBM thickening. As shown in Figure 2A, an expanded glomerular tuft area and marked GBM thickening were observed in diabetic mice compared to normal control mice. However, treatment with two doses of RAP ameliorated these changes.

TGF-β1 is considered to be one of the vital mediators of excessive ECM deposition in DN, which results in glomerulosclerosis.[30] CTGF expression is induced by TGF-β1, which contributes to its downstream profibrotic effects.[31] We performed immunohistochemistry to evaluate the expression of TGF-β1 and CTGF in glomeruli of diabetic mice. The C57BL/6 mice induced by STZ significantly increased the positive staining of TGF-β1 and CTGF in the glomeruli compared to the normal control mice. However, glomerular staining of TGF-β1 and CTGF was effectively abrogated in diabetic mice treated with RAP (Figure 2A–C). In addition, mRNA expression levels of CTGF and TGF-β1 were detected in parallel by RT-PCR using whole kidney cortex. As shown in Figure 2D and E, the mRNA expression levels of CTGF and TGF-β1 were prominently increased in diabetic kidneys but were dramatically decreased in diabetic kidneys treated with RAP.

RAP alleviates collagen deposition, ECM accumulation, and α-SMA expression in diabetic mice

Histologically, changes in collagen accumulation, which indicate the development of fibrosis in renal tissue, were visualized with Sirius red (red color) and Masson's trichrome staining (blue color). As shown in Figure 3, the above two experimental methods showed marked collagen deposition in STZ-induced mouse kidneys, and less deposition in low- and high-dose RAP-treated mouse kidneys.

Furthermore, immunohistochemistry, Western blotting, and RT-PCR analysis were used to examine the mRNA and protein levels of FN, an ECM protein in diabetic mouse kidney tissues. The results showed a remarkably higher level of FN in diabetic mice than in control mice. This was consistent with the mRNA expression levels. FN expression levels were also significantly decreased in diabetic mice treated with low and high doses of RAP (Figure 3A, D, F, and G). These results revealed that RAP treatment attenuated ECM synthesis in diabetic renal tissues. Expression of α-SMA in the renal areas becomes upregulated with ECM accumulation, and this is thought to indicate changes in myofibroblasts.[32,33] To explore the mechanisms of renal fibrosis amelioration, we examined the effect of RAP on α-SMA expression. The results showed that α-SMA expression was markedly enhanced in the kidney after STZ injection by immunohistochemical analysis (Figure 3A and E), Western blot (Figure 3F), and RT-PCR analysis (Figure 3H). Upregulation of α-SMA expression was significantly ameliorated in high-dose RAP-treated kidneys compared to control
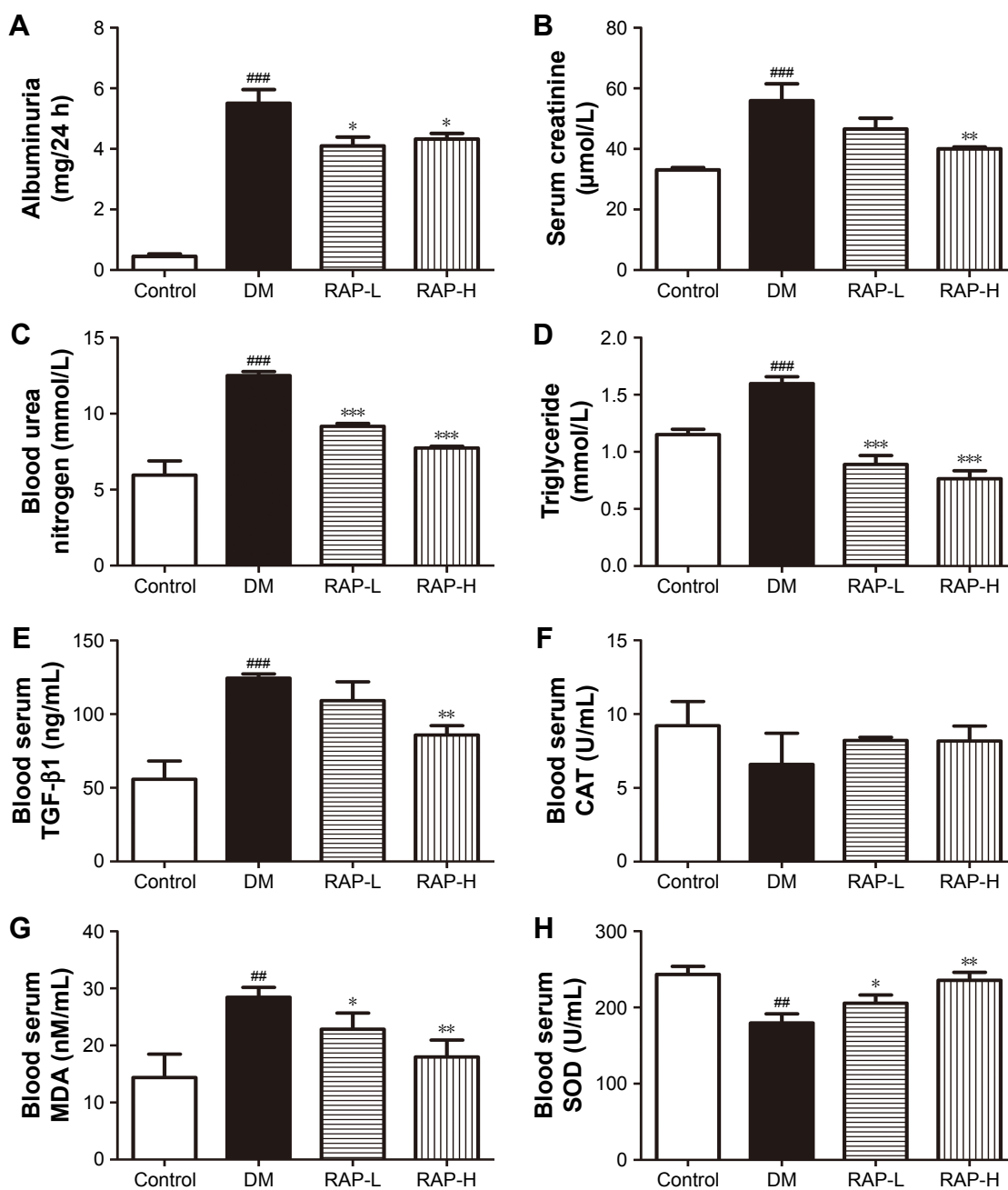
Figure 1 RAP ameliorates biochemical indices, serum TGF-β1 levels, and oxidative stress parameters in diabetic mice.
Notes: The relative amount of (**A**) 24-hour albuminuria, (**B**) serum creatinine, (**C**) blood urea nitrogen, (**D**) triglyceride, (**E**) TGF-β1, (**F**) CAT, (**G**) MDA, and (**H**) SOD in the serum of mice. Data are presented as the mean ± SD, n=8. $^{\#\#}p<0.01$ and $^{\#\#\#}p<0.001$ versus control mice; $^{*}p<0.05$, $^{**}p<0.01$, and $^{***}p<0.001$ versus DM.
Abbreviations: CAT, catalase; DM, diabetic model; MDA, malondialdehyde; RAP-H, high-dose RAP; RAP-L, low-dose RAP; SOD, superoxide dismutase; TGF-β1, transforming growth factor-β1.

kidneys, whereas low-dose RAP treatment had no effect on α-SMA expression.

RAP alleviates MAPK and NF-κB signaling pathways in diabetic mice

Next, we demonstrated the protective mechanisms of RAP against renal fibrosis. Previous studies have shown that phosphorylation of MAPKs is upregulated in the kidneys of STZ-induced diabetic rats.[34] Hence, we assessed the role of RAP

treatment on MAPK activation by examining the phosphorylation of ERK1/2 and p38 using immunohistochemical analysis. The results showed that the positive areas of phosphorylated ERK1/2 and p38 staining were markedly increased in STZ-induced diabetic kidneys compared to normal control kidneys. However, treatment with RAP at dosages of 0.1 and 0.5 mg/kg decreased the expression levels of p-ERK1/2 and p-p38 in renal tissue (Figure 4A–C). NF-κB is expressed in various tissues, and it serves as a vital molecule in mediating inflammation and
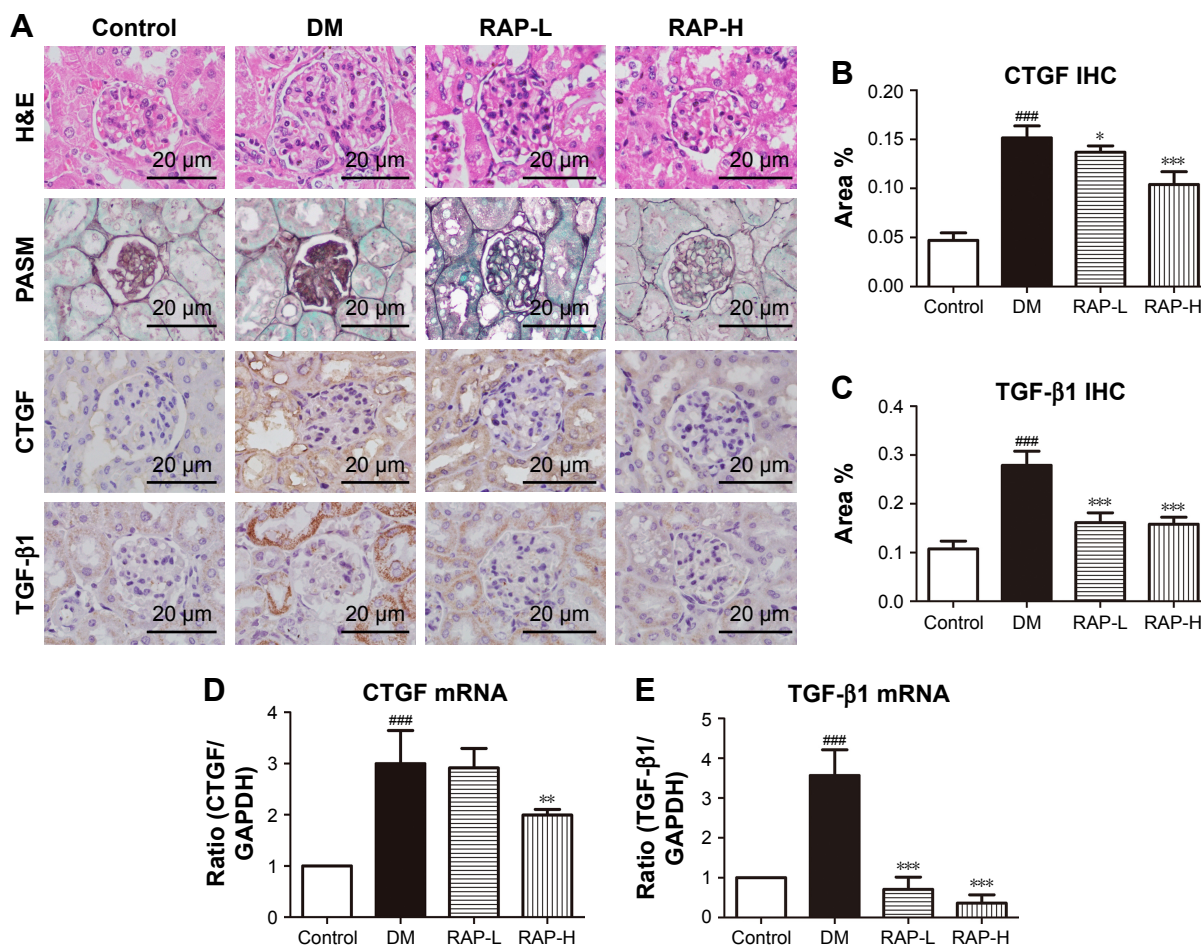
Figure 2 RAP inhibits the glomerular hypertrophy and glomerular basement membrane thickening in diabetic mice.

Notes: (**A**) Kidney sections were stained with PASM and H&E staining as well as immunohistochemical staining of CTGF and TGF-β1 (original magnifications, ×400). The staining of (**B**) CTGF and (**C**) TGF-β1 in mouse kidney were quantified. The mRNA levels of (**D**) CTGF and (**E**) TGF-β1 were analyzed by reverse transcriptase polymerase chain reaction. Data are presented as the mean ± SD, n=8. ###$p<0.001$ versus control mice; *$p<0.05$, **$p<0.01$, and ***$p<0.001$ versus DM.

Abbreviations: CTGF, connective tissue growth factor; DM, diabetic model; IHC, immunohistochemistry; PASM, periodic acid-silver methenamine; RAP-H, high-dose RAP; RAP-L, low-dose RAP; TGF-β1, transforming growth factor-β1.

fibrosis in DN.[35] We measured the level of NF-κB p65 subunit phosphorylation in the kidneys of the four experimental groups by immunohistochemical analysis. As shown in Figure 4D, p-p65 expression in diabetic mice was significantly upregulated compared to that in normal control mice. In contrast, treatment with RAP reversed these changes by inhibiting the expression of p-p65. For further verification, we examined the phosphorylation of ERK1/2, p38 and p65 by Western blot analysis. The results of the Western blot experiment agreed with immunohistochemical analysis (Figure 4E-H). This suggests that MAPK and NF-κB signaling pathways underlie the alleviation of diabetic renal fibrosis by RAP.

In vitro experiments
RAP inhibits HG-induced ECM accumulation in cell culture medium and MC proliferation
MC is considered to be a crucial factor leading to glomerular sclerosis in diabetic patients.[36] To determine the effective

concentrations of RAP for the treatment of MCs, five concentrations of RAP (10, 50, 100, 150, and 200 µM) were used to treat MCs, and cell proliferation induced by HG was evaluated using the MTT assay. The results showed that the proliferation of MCs was increased under HG conditions compared to NG conditions. However, RAP significantly inhibited the proliferation of MCs from the concentration of 50 µM (Figure 5A). To verify whether the inhibition of proliferation by RAP is related to its toxicity, we examined the cytotoxicity of RAP at these five concentrations in MCs. Interestingly, RAP produced no toxicity in MCs at these five concentrations (Figure 5B), indicating that RAP can inhibit the proliferation of MCs without cytotoxicity. Based on these results, we selected 50 and 100 µM for RAP concentrations in our subsequent experiments.

To examine whether RAP could suppress the excessive expression of FN and COL4 in HG-induced MCs, we measured the levels of FN and COL4 in the supernatant
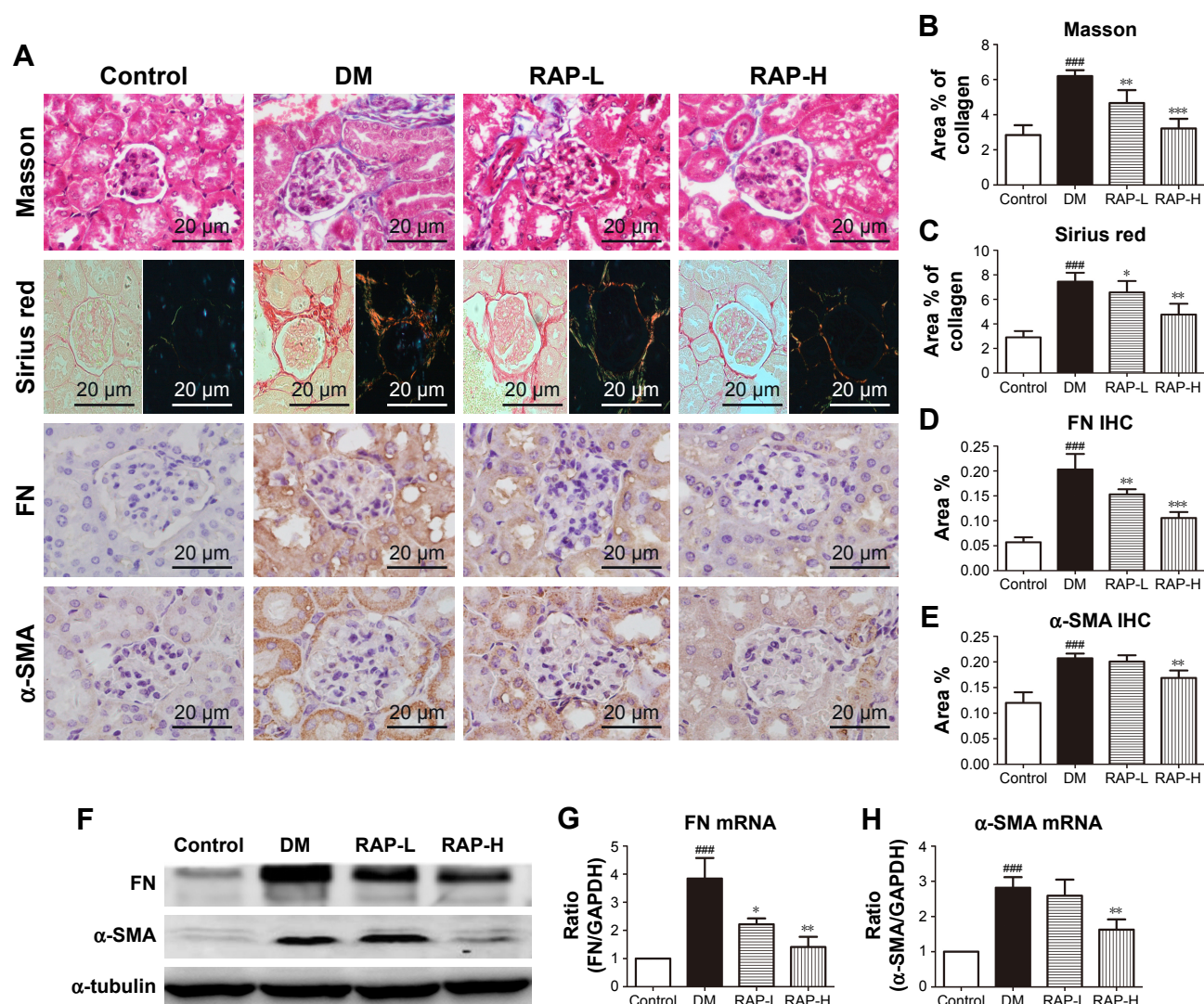
Figure 3 RAP alleviates collagen deposition, ECM accumulation, and α-SMA expression in diabetic mice.
Notes: (**A**) Representative renal sections were stained with Masson-trichrome and Sirius red along with immunohistochemical staining of FN and α-SMA (original magnifications, ×400). Quantitative analysis of the results for fibrotic area stained with (**B**) Masson and (**C**) Sirius red in mouse kidneys. The positive areas of (**D**) FN and (**E**) α-SMA staining were quantified. (**F**) The protein and mRNA expressions of (**G**) FN and (**H**) α-SMA were measured by Western blot and reverse transcriptase polymerase chain reaction. Data are presented as the mean ± SD, n=8. ###$p<0.001$ versus control mice; *$p<0.05$, **$p<0.01$, and ***$p<0.001$ versus DM.
Abbreviations: DM, diabetic model; FN, fibronectin; IHC, immunohistochemistry; RAP-H, high-dose; RAP-L, low-dose RAP; α-SMA, α-smooth muscle actin.

of MCs using ELISA analysis. As we expected, the results demonstrated that RAP significantly attenuated the excessive production of COL4 and FN in MCs induced by HG (Figure 5C and D). These results suggest that RAP could suppress excessive HG-induced ECM accumulation in MCs, thus inhibiting renal fibrosis.

RAP prevents HG-induced intracellular ECM accumulation and MAPK/NF-κB signaling pathways in MCs

In our study, the ECM accumulation markers FN, TGF-β1, CTGF, and α-SMA induced by HG in MCs were detected

by Western blot and RT-PCR analysis. The results showed that the protein and mRNA levels of FN, TGF-β1, CTGF, and α-SMA in the HG-induced group were higher than those in the NG group. Interestingly, after 48 h of treatment by RAP at two concentrations, these changes were weakened (Figure 6A–E). Given the role of MAPK and NF-κB signaling in MC growth and proliferation, which contribute to ECM accumulation, we further investigated the signaling cascade between HG-induced ECM accumulation and MAPK/NF-κB pathways. HG induced MAPK and NF-κB activation, as manifested by the fact that the relative amounts of phosphorylated p-ERK1/2, p38, and p65 were observably
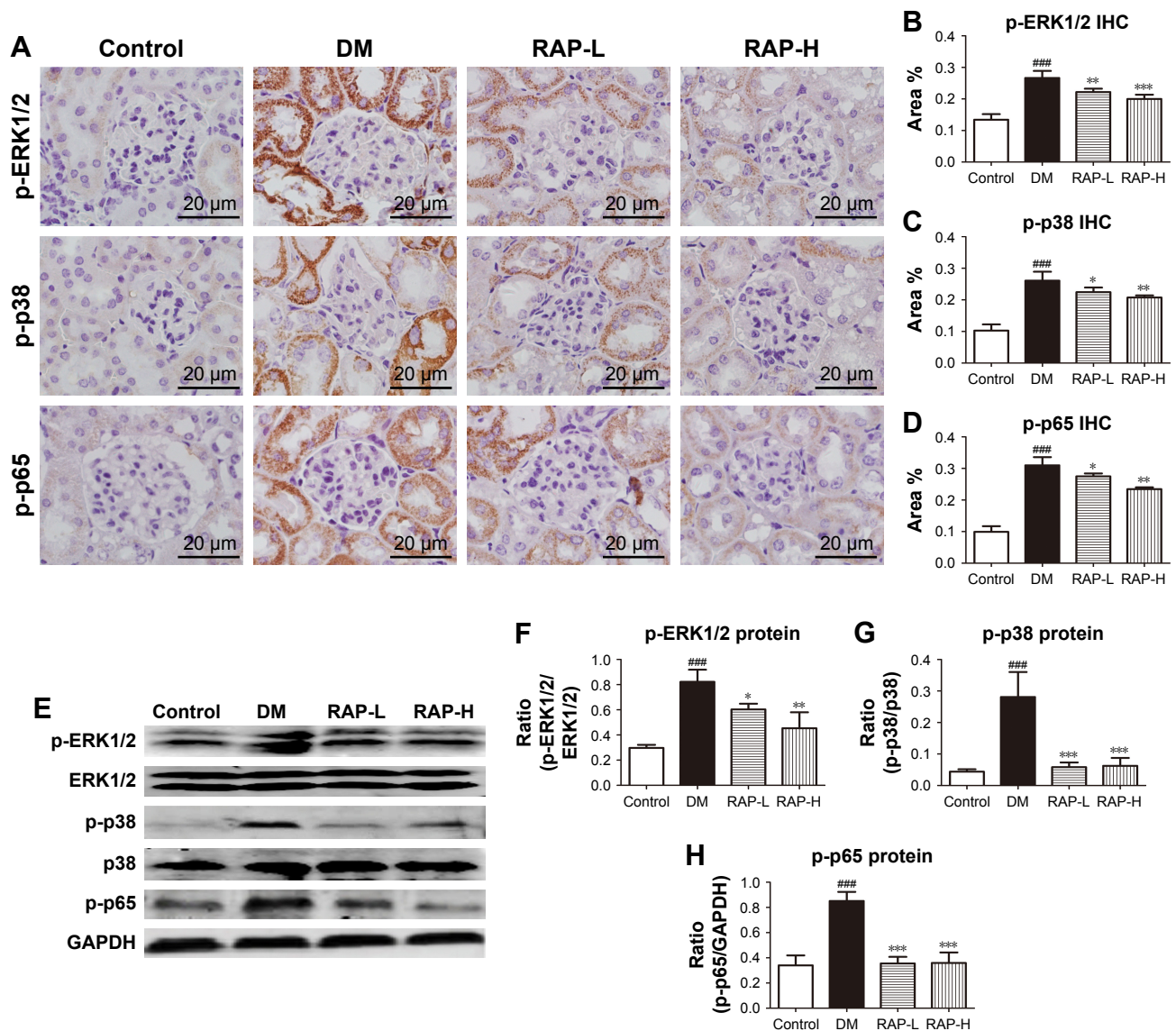
Figure 4 RAP alleviates mitogen-activated protein kinase and nuclear factor κB signaling pathways in diabetic mice.
Notes: (**A**) The expression levels of phosphorylated ERK1/2, p38, and p65 were determined by immunohistochemical staining (original magnifications, ×400). The staining of (**B**) p-ERK1/2, (**C**) p-p38, and (**D**) p-p65 were quantified. (**E**) ERK1/2, p38, p65, and their phosphorylation levels were measured by Western blot analysis. (**F**, **G** and **H**) Densitometric quantification of phosphorylated ERK1/2 and p38 to total ERK1/2 and p38, respectively, and p-p65 to GAPDH are summarized. Data are presented as the mean ± SD, n=8. ###$p < 0.001$ versus control mice; *$p < 0.05$, **$p < 0.01$, and ***$p < 0.001$ versus DM.
Abbreviations: DM, diabetic model; GAPDH, glyceraldehyde-3-phosphate dehydrogenase; IHC, immunohistochemistry; RAP-H, high-dose RAP; RAP-L, low-dose RAP.

increased compared to normal control cells. However, RAP therapy effectively reduced the HG-induced phosphorylation of ERK1/2, p38, and p65 in MCs at concentrations of 50 and 100 μM (Figure 6F–I). These findings indicate that RAP alleviates HG-induced ECM accumulation by suppressing the MAPK and NF-κB signaling pathways.

Discussion

The present study demonstrated that the peptide RAP, which is derived from rapeseed protein, could protect against

STZ-induced renal fibrosis in mice. Furthermore, RAP treatment significantly attenuated ECM deposition in vivo and in vitro. Finally, RAP may inhibit renal fibrosis by modulating the MAPK and NF-κB signaling pathways.

BW loss is usually observed in short- and long-term experimental diabetes studies. BW loss in diabetic mice was found to be related to muscle loss due to hyperglycemia-induced over-catabolism of tissue proteins. We detected significant weight loss in the diabetic group compared to the control group, which was consistent with the results of a previous study.[37]
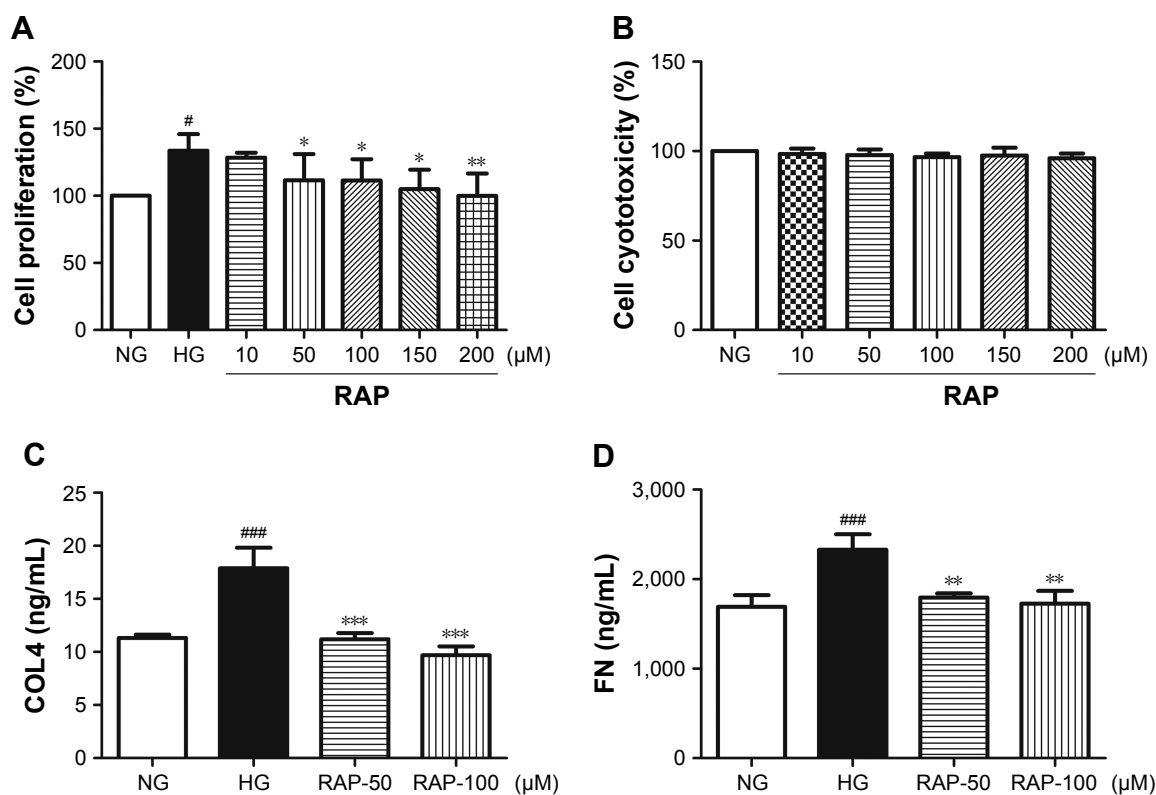
Figure 5 RAP inhibits HG-induced ECM accumulation in cell culture medium and MCs proliferation.
Notes: (**A**) MCs were cultured with NG DMEM or HG DMEM or HG DMEM with different concentrations of RAP (10, 50, 100, 150, and 200 μM), respectively. (**B**) MCs were treated with NG DMEM cultured in the presence or absence of indicated concentrations of RAP and cell viability was measured by MTT. (**C** and **D**) The levels of COL4 and FN in the supernatant of MCs were determined by enzyme-linked immunosorbent assay analysis. Data are presented as the mean ± SD. #$p < 0.05$ and ###$p < 0.001$ versus NG; *$p < 0.05$, **$p < 0.01$, and ***$p < 0.001$ versus HG.
Abbreviations: COL4, collagen 4; ECM, extracellular matrix; FN, fibronectin; HG, high glucose; MCs, mesangial cells; NG, normal glucose.

Administration of RAP markedly improved the loss of BW. Furthermore, we found that RAP markedly ameliorated the renal function indices BUN, Cr, and triglycerides. However, treatment with RAP for 12 weeks had no effect on FBG levels in diabetic mice, suggesting that RAP can protect the kidneys, but it does not affect hypoglycemia.

Albuminuria has been shown to be a good clinical predictor of renal lesions in DN.[38] Severe albuminuria reflects the presence of major glomerular lesions that trigger progressive glomerulosclerosis. A previous study revealed that albumin excretion in STZ-induced mice fed a HFD was elevated by fourfold at 8 weeks compared to that in normal mice.[39] In our present study, the 24-h albuminuria of STZ+HFD mice was increased by up to tenfold at 12 weeks compared to that of control mice. This suggested that the kidney injury was more severe at 12 weeks than at 8 weeks in diabetic mice. Interestingly, RAP treatment at both low and high doses significantly reduced 24-h albumin excretion in diabetic mice.

Increased accumulation of ECM is the main characteristic of renal fibrosis in renal tissue.[40,41] FN, an important component of the ECM, is thought to be a critical factor in the differentiation of myofibroblasts, which are characterized by α-SMA expression. Our results revealed that FN and α-SMA expression is potently inhibited in diabetic kidneys and HG-induced MCs by RAP treatment. TGF-β is a crucial mediator of ECM accumulation, which induces the expression of CTGF in different tissues. The importance of CTGF in renal disease has been studied in the unilateral ureteral obstruction (UUO) model of renal fibrosis[11] and in type 1 and type 2 diabetes.[42] Several reports have shown that CTGF can induce EMT in proximal tubular epithelial cells and that this effect is independent of the presence of TGF-β. Moreover, together, these two growth factors can provide a powerful signal for EMT.[43] CTGF has been shown to bind to TGF-β1 to activate phosphorylation of smad2.[44] These findings suggest that CTGF may transduce its signals partly by binding to TGF-β1. Interestingly, our study showed that RAP markedly attenuated CTGF and TGF-β1 expression in diabetic mouse kidney and MCs in response to HG. All these data indicate that RAP suppresses ECM accumulation by inhibiting the expression of TGF-β1 and its downstream factor CTGF.
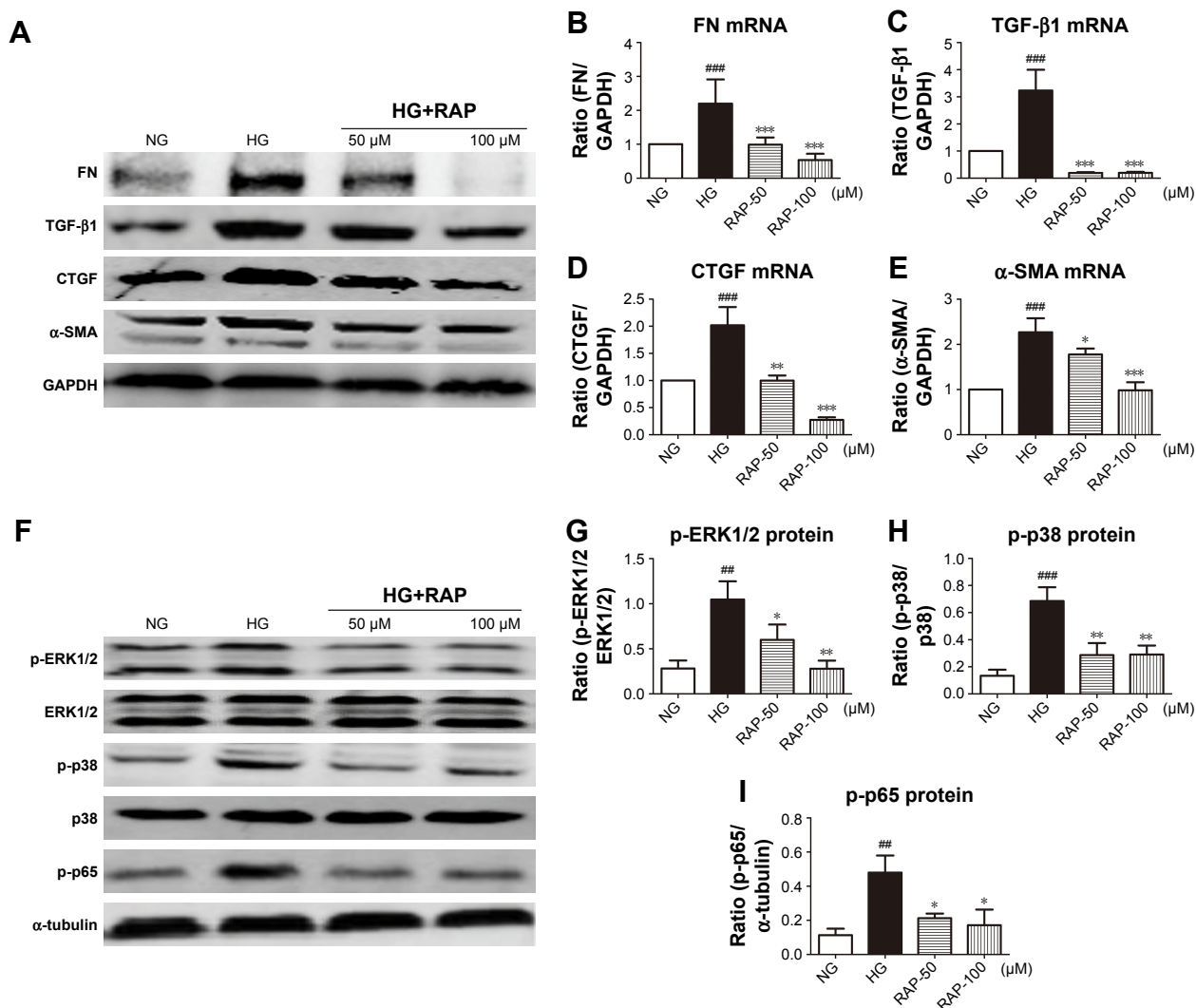
Figure 6 RAP prevents HG-induced intracellular ECM accumulation and mitogen-activated protein kinase/nuclear factor κB signaling pathways in mesangial cells.
Notes: (**A**) The protein expressions of FN, TGF-β1, CTGF, and α-SMA were measured by Western blot. The mRNA levels of (**B**) FN, (**C**) TGF-β1, (**D**) CTGF, and (**E**) α-SMA in mesangial cells were assessed by reverse transcriptase polymerase chain reaction. (**F**) The phosphorylation of ERK1/2, p38, and p65 in mesangial cells was examined by Western blot. (**G–I**) Densitometric quantification of phosphorylated ERK1/2 and p38 to total ERK1/2 and p38, respectively, or p-p65 compared to α-tubulin was summarized. Data are presented as the mean ± SD. ##$p < 0.01$ and ###$p < 0.001$ versus NG; *$p < 0.05$, **$p < 0.01$, and ***$p < 0.001$ versus HG.
Abbreviations: CTGF, connective tissue growth factor; ECM, extracellular matrix; FN, fibronectin; HG, high glucose; NG, normal glucose; α-SMA, α-smooth muscle actin; TGF-β1, transforming growth factor-β1.

As RAP has a therapeutic effect on renal fibrosis in DN, what is the molecular mechanism by which RAP affects renal fibrosis? We studied two important signaling pathways in DN: MAPK and NF-κB. MAPKs, particularly ERK1/2 and p38, are a family of serine/threonine kinases. Activation of the MAPK signaling pathway has been shown to occur in rats with diabetes and renal fibrosis.[45] MAPK inhibitors play an important role in TGF-β1-induced ECM synthesis and in the phenotypic transformation of MCs, which eventually lead to renal fibrosis in diabetes. Increasing evidence suggests that the expression of α-SMA decreased significantly when p38 MAPK is blocked by the specific blocker SB203580.[46] Furthermore, previous study demonstrated that the p38

MAPK signaling pathway was activated by HG stimulation in human renal tubular epithelial cells.[47] In this study, we found that phosphorylation of p38 and ERK1/2 was increased by HG stimulation in MCs and in HFD+STZ-induced diabetic mouse kidneys. This was consistent with increased FN and α-SMA synthesis. However, these changes were attenuated by RAP treatment. The positive relationship of p-ERK1/2, p-p38, and FN with α-SMA overproduction indicates that RAP may restrain renal fibrosis by inhibiting the MAPK pathway.

NF-κB is a nuclear transcription factor with multidirectional regulation that regulates a variety of inflammatory cytokines, chemokines, and fibrosis factors. It participates in cell

proliferation and ECM deposition, playing an important role in DN. Moreover, previous studies have shown that MAPK has numerous direct and indirect interactions with NF-κB.[48–50] Activated ERK and p38 MAPK pathways are thought to be the physiologic activators of NF-κB.[51,52] Another previous study showed that the activation of NF-κB is enhanced in the kidneys of diabetic animals, which augments the expansion of mesangium. Increasing evidence suggests that NF-κB plays a pivotal role in all pathophysiologic environments in which fibrosis is a pivotal event.[18] In addition, most of the current experimental and clinical methods to slow the progression of fibrosis in DN, such as thiazolidinedione,[53] angiotensin system inhibitors,[54] and pyrrolidine dithiocarbamate,[55] are known to modulate NF-κB. All these results indicate that the activation of NF-κB may be an important link in the development of renal fibrosis. Furthermore, the data showed that the COL4 deposition and α-SMA and FN expression were decreased after the inhibition of NF-κB activity in UUO rats.[56] In this study, we observed that RAP could affect the NF-κB signaling pathway and regulate the fibrotic components. Under HG conditions, RAP attenuated the phosphorylation of NF-κB p65 and its downstream gene TGF-β1 and FN in a dose-dependent manner. In vivo, experimental results were similar to in vitro experimental results. Thus, these results demonstrated that RAP improved renal fibrosis and ECM accumulation by inhibiting the NF-κB signaling pathway.

Given that RAP has a good therapeutic effect on renal fibrosis but no hypoglycemic effect on DN mice, we considered using RAP in other fibrosis models. Therefore, future studies are still warranted to identify whether RAP has a therapeutic effect on renal interstitial fibrosis (UUO) animal models to achieve a better therapeutic effect.

Conclusion

In conclusion, the peptide RAP alleviates renal fibrosis in DN by suppressing the MAPK and NF-κB pathways. In subsequent research, RAP is expected to be designed as a leading compound for drugs to treat renal fibrosis. More importantly, this study demonstrated for the first time that plant-derived bioactive peptides in foodstuffs inhibited fibrosis in DN and glomerular MCs. This finding serves as a basis for future studies of treatment for renal fibrosis using bioactive peptides in plant-derived foodstuffs.

Although this study put forward a new idea that plant-derived bioactive peptides in foodstuffs inhibited fibrosis in DN and MCs, only one of these peptides has been studied. Thus, many basic and clinical experiments are still needed to verify the anti-renal fibrosis effect of these types of peptides.

More importantly, in future research, we will optimize RAP's structure according to its physical and chemical properties, pharmacokinetic, adverse reactions, and side effects, to make it a leading compound for drugs to treat renal fibrosis.

Disclosure

The authors report no conflicts of interest in this work.

References

1. Decleves AE, Sharma K. New pharmacological treatments for improving renal outcomes in diabetes. *Nat Rev Nephrol*. 2010;6(6):371–380.
2. Balakumar P, Arora MK, Reddy J, Anand-Srivastava MB. Pathophysiology of diabetic nephropathy: involvement of multifaceted signalling mechanism. *J Cardiovasc Pharmacol*. 2009;54(2):129–138.
3. Choudhury D, Tuncel M, Levi M. Diabetic nephropathy – a multifaceted target of new therapies. *Disco Med*. 2010;10(54):406–415.
4. Sutariya B, Jhonsa D, Saraf MN. TGF-beta: the connecting link between nephropathy and fibrosis. *Immunopharmacol Immunotoxicol*. 2016;38(1):39–49.
5. Brosius FC, Khoury CC, Buller CL, Chen S. Abnormalities in signaling pathways in diabetic nephropathy. *Expert Rev Endocrinol Metab*. 2010;5(1):51–64.
6. Ziyadeh FN. The extracellular matrix in diabetic nephropathy. *Am J Kidney Dis*. 1993;22(5):736–744.
7. Liu Y. New insights into epithelial-mesenchymal transition in kidney fibrosis. *J Am Soc Nephrol*. 2010;21(2):212–222.
8. Chen S, Hong SW, Iglesias-de la Cruz MC, Isono M, Casaretto A, Ziyadeh FN. The key role of the transforming growth factor-beta system in the pathogenesis of diabetic nephropathy. *Ren Fail*. 2001;23(3–4):471–481.
9. Riser BL, Denichilo M, Cortes P, et al. Regulation of connective tissue growth factor activity in cultured rat mesangial cells and its expression in experimental diabetic glomerulosclerosis. *J Am Soc Nephrol*. 2000;11(1):25–38.
10. Wahab NA, Yevdokimova N, Weston BS, et al. Role of connective tissue growth factor in the pathogenesis of diabetic nephropathy. *Biochem J*. 2001;359(Pt 1):77–87.
11. Yokoi H, Mukoyama M, Nagae T, et al. Reduction in connective tissue growth factor by antisense treatment ameliorates renal tubulointerstitial fibrosis. *J Am Soc Nephrol*. 2004;15(6):1430–1440.
12. Mehdi UF, Adams-Huet B, Raskin P, Vega GL, Toto RD. Addition of angiotensin receptor blockade or mineralocorticoid antagonism to maximal angiotensin-converting enzyme inhibition in diabetic nephropathy. *J Am Soc Nephrol*. 2009;20(12):2641–2650.
13. Ma FY, Sachchithananthan M, Flanc RS, Nikolic-Paterson DJ. Mitogen activated protein kinases in renal fibrosis. *Front Biosci (Schol Ed)*. 2009;1:171–187.
14. Cheng X, Gao W, Dang Y, et al. Both ERK/MAPK and TGF-Beta/Smad signaling pathways play a role in the kidney fibrosis of diabetic mice accelerated by blood glucose fluctuation. *J Diabetes Res*. 2013;2013:463740.

15. Rhyu DY, Yang Y, Ha H, et al. Role of reactive oxygen species in TGF-beta1-induced mitogen-activated protein kinase activation and epithelial-mesenchymal transition in renal tubular epithelial cells. *J Am Soc Nephrol*. 2005;16(3):667–675.

16. Santibanez JF. JNK mediates TGF-beta1-induced epithelial mesenchymal transdifferentiation of mouse transformed keratinocytes. *FEBS Lett*. 2006;580(22):5385–5391.

17. Xie L, Law BK, Chytil AM, Brown KA, Aakre ME, Moses HL. Activation of the Erk pathway is required for TGF-beta1-induced EMT in vitro. *Neoplasia*. 2004;6(5):603–610.

18. Tamada S, Asai T, Kuwabara N, et al. Molecular mechanisms and therapeutic strategies of chronic renal injury: the role of nuclear factor κB activation in the development of renal fibrosis. *J Pharm Sci*. 2006;100(1):17–21.

19. Giunti S, Tesch GH, Pinach S, et al. Monocyte chemoattractant protein-1 has prosclerotic effects both in a mouse model of experimental diabetes and in vitro in human mesangial cells. *Diabetologia*. 2008;51(1):198–207.

20. Xie X, Peng J, Chang X, et al. Activation of RhoA/ROCK regulates NF-kappaB signaling pathway in experimental diabetic nephropathy. *Mol Cell Endocrinol*. 2013;369(1–2):86–97.

21. Gaede P, Lund-Andersen H, Parving HH, Pedersen O. Effect of a multifactorial intervention on mortality in type 2 diabetes. *N Engl J Med*. 2008;358(6):580–591.

22. Maestri E, Marmiroli M, Marmiroli N. Bioactive peptides in plant-derived foodstuffs. *J Proteomics*. 2016;147:140–155.

23. Pang G, Xie J, Chen Q, Hu Z. How functional foods play critical roles in human health. *Food Sci Hum Wellness*. 2012;1(1):26–60.

24. Chi CF, Hu FY, Wang B, Li T, Ding GF. Antioxidant and anticancer peptides from the protein hydrolysate of blood clam (Tegillarca granosa) muscle. *J Funct Foods*. 2015;15:301–313.

25. Fang X, Xie N, Chen X, Yu H, Chen J. Optimization of antioxidant hydrolysate production from flying squid muscle protein using response surface methodology. *Food Bioprod Process*. 2012;90(4):676–682.

26. McClean S, Beggs LB, Welch RW. Antimicrobial activity of antihypertensive food-derived peptides and selected alanine analogues. *Food Chem*. 2014;146:443–447.

27. Xie N, Wang B, Jiang L, Liu C, Li B. Hydrophobicity exerts different effects on bioavailability and stability of antioxidant peptide fractions from casein during simulated gastrointestinal digestion and Caco-2 cell absorption. *Food Res Int*. 2015;76(Pt 3):518–526.

28. Xu F, Wang L, Ju X, et al. Transepithelial transport of YWDHNNPQIR and its metabolic fate with cytoprotection against oxidative stress in human intestinal Caco-2 cells. *J Agric Food Chem*. 2017;65(10):2056–2065.

29. Craven PA, Melhem MF, Phillips SL, DeRubertis FR. Overexpression of Cu2+/Zn2+ superoxide dismutase protects against early diabetic glomerular injury in transgenic mice. *Diabetes*. 2001;50(9):2114–2125.

30. Schena FP. Pathogenetic mechanisms of diabetic nephropathy. *J Am Soc Nephrol*. 2005;16 (Suppl 1):S30–S33.

31. Montford JR, Furgeson SB. A new CTGF target in renal fibrosis. *Kidney Int*. 2017;92(4):784–786.

32. Desmouliere A, Geinoz A, Gabbiani F, Gabbiani G. Transforming growth factor-beta 1 induces alpha-smooth muscle actin expression in granulation tissue myofibroblasts and in quiescent and growing cultured fibroblasts. *J Cell Biol*. 1993;122(1):103–111.

33. Muller GA, Rodemann HP. Characterization of human renal fibroblasts in health and disease: I. Immunophenotyping of cultured tubular epithelial cells and fibroblasts derived from kidneys with histologically proven interstitial fibrosis. *Am J Kidney Dis*. 1991;17(6):680–683.

34. Jiao Z, Chen J, Liu Y, Liu T, Chen K, Li G. Role of ERK1/2 and JNK phosphorylation in iodine contrast agent-induced apoptosis in diabetic rat kidneys. *Renal Fail*. 2015;37(8):1349–1355.

35. Yi B, Hu X, Zhang H, et al. Nuclear NF-kappaB p65 in peripheral blood mononuclear cells correlates with urinary MCP-1, RANTES and the severity of type 2 diabetic nephropathy. *PLoS One*. 2014;9(6):e99633.

36. Striker GE, Peten EP, Carome MA, et al. The kidney disease of diabetes mellitus (KDDM): a cell and molecular biology approach. *Diabetes Metab Rev*. 1993;9(1):37–56.

37. Sutariya B, Saraf M. Betanin, isolated from fruits of Opuntia elatior Mill attenuates renal fibrosis in diabetic rats through regulating oxidative stress and TGF-beta pathway. *J Ethnopharmacol*. 2017;198:432–443.

38. Schlatzer DM, Dazard JE, Dharsee M, et al. Urinary protein profiles in a rat model for diabetic complications. *Mol Cell Proteomics*. 2009;8(9):2145–2158.

39. Ji X, Li C, Ou Y, et al. Andrographolide ameliorates diabetic nephropathy by attenuating hyperglycemia-mediated renal oxidative stress and inflammation via Akt/NF-kappaB pathway. *Mol Cell Endocrinol*. 2016;437:268–279.

40. Qian Y, Feldman E, Pennathur S, Kretzler M, Brosius FC 3rd. From fibrosis to sclerosis: mechanisms of glomerulosclerosis in diabetic nephropathy. *Diabetes*. 2008;57(6):1439–1445.

41. Satriano J. Kidney growth, hypertrophy and the unifying mechanism of diabetic complications. *Amino Acids*. 2007;33(2):331–339.

42. Guha M, Xu ZG, Tung D, Lanting L, Natarajan R. Specific down-regulation of connective tissue growth factor attenuates progression of nephropathy in mouse models of type 1 and type 2 diabetes. *FASEB J*. 2007;21(12):3355–3368.

43. Cheng O, Thuillier R, Sampson E, et al. Connective tissue growth factor is a biomarker and mediator of kidney allograft fibrosis. *Am J Transplant*. 2006;6(10):2292–2306.

44. Abreu JG, Ketpura NI, Reversade B, De Robertis EM. Connective-tissue growth factor (CTGF) modulates cell signalling by BMP and TGF-beta. *Nat Cell Biol*. 2002;4(8):599–604.

45. Ding Z, Chen Z, Chen X, et al. Adenovirus-mediated anti-sense ERK2 gene therapy inhibits tubular epithelial-mesenchymal transition and ameliorates renal allograft fibrosis. *Transpl Immunol*. 2011;25(1):34–41.

46. Chin BY, Mohsenin A, Li SX, Choi AM, Choi ME. Stimulation of pro-alpha(1)(I) collagen by TGF-beta(1) in mesangial cells: role of the p38 MAPK pathway. *Am J Physiol Renal Physiol*. 2001;280(3):F495–F504.

47. Lv ZM, Wang Q, Wan Q, et al. The role of the p38 MAPK signaling pathway in high glucose-induced epithelial-mesenchymal transition of cultured human renal tubular epithelial cells. *PLoS One*. 2011;6(7):e22806.

48. Carter AB, Knudtson KL, Monick MM, Hunninghake GW. The p38 mitogen-activated protein kinase is required for NF-kappaB-dependent gene expression. The role of TATA-binding protein (TBP). *J Biol Chem*. 1999;274(43):30858–30863.

49. Grund EM, Kagan D, Tran CA, et al. Tumor necrosis factor-alpha regulates inflammatory and mesenchymal responses via mitogen-activated protein kinase kinase, p38, and nuclear factor kappaB in human endometriotic epithelial cells. *Mol Pharmacol*. 2008;73(5):1394–1404.

50. Saccani S, Pantano S, Natoli G. p38-Dependent marking of inflammatory genes for increased NF-kappa B recruitment. *Nat Immunol*. 2002;3(1):69–75.

51. Je JH, Lee JY, Jung KJ, et al. NF-kappaB activation mechanism of 4-hydroxyhexenal via NIK/IKK and p38 MAPK pathway. *FEBS Lett*. 2004;566(1–3):183–189.

52. Jiang B, Xu S, Hou X, Pimentel DR, Brecher P, Cohen RA. Temporal control of NF-kappaB activation by ERK differentially regulates interleukin-1beta-induced gene expression. *J Biol Chem*. 2004;279(2):1323–1329.

53. Ohga S, Shikata K, Yozai K, et al. Thiazolidinedione ameliorates renal injury in experimental diabetic rats through anti-inflammatory effects mediated by inhibition of NF-kappaB activation. *Am J Physiol Renal Physiol*. 2007;292(4):F1141–F1150.

54. Lee FT, Cao Z, Long DM, et al. Interactions between angiotensin II and NF-kappaB-dependent pathways in modulating macrophage infiltration in experimental diabetic nephropathy. *J Am Soc Nephrol*. 2004;15(8):2139–2151.

55. Tashiro K, Tamada S, Kuwabara N, et al. Attenuation of renal fibrosis by proteasome inhibition in rat obstructive nephropathy: possible role of nuclear factor kappaB. *Int J Mol Med*. 2003;12(4):587–592.

56. Nakatani T, Tamada S, Asai T, et al. Role of renin-angiotensin system and nuclear factor-kappaB in the obstructed kidney of rats with unilateral ureteral obstruction. *Jpn J Pharmacol*. 2002;90(4):361–364.